Aerosol and Air Quality Research, 16: 2368–2377, 2016

ISSN: 1680-8584 print / 2071-1409 online
doi: 10.4209/aaqr.2015.11.0632

Atmospheric CO, O_3, and SO_2 Measurements at the Summit of Mt. Fuji during the Summer of 2013

Shungo Kato[1*], Yasuhiro Shiobara[1], Katsumi Uchiyama[1], Kazuhiko Miura[2], Hiroshi Okochi[3], Hiroshi Kobayashi[4], Shiro Hatakeyama[5]

[1] *Department of Applied Chemistry, Faculty of Urban Environmental Sciences, Tokyo Metropolitan University, Tokyo 192-0397, Japan*
[2] *Department of Physics, Faculty of Science, Tokyo University of Science, Tokyo 162-8601, Japan*
[3] *Graduate School of Science and Engineering, Waseda University, Tokyo 169-8555, Japan*
[4] *Department of Ecosocial System Engineering, University of Yamanashi, Yamanashi 400-8510, Japan*
[5] *Department of Environmental and Natural Resource Science, Faculty of Agriculture, Tokyo University of Agriculture and Technology, Tokyo 183-8509, Japan*

ABSTRACT

Atmospheric trace gases CO, O_3, and SO_2 were observed at the summit of Mt. Fuji (3776 m a.s.l.) during the summer of 2013. Considerable variations were observed in the concentrations of CO and O_3; however, they were correlated in most cases. Trends analyzed through backward trajectory calculations showed lower concentrations of CO and O_3 transported from the Pacific Ocean and South East Asia directions, while higher concentrations were detected from the direction of the Asian continent. High O_3 and low CO concentrations were observed during some periods; in these air masses, water content of the air was low indicating that the air originated from high altitudes and was influenced by the stratosphere. Gaseous SO_2 was mostly lower than the detection limit of the instrument used for measurement (0.06 ppbv), but on August 20–21, high SO_2 spikes of about 5 ppbv were observed. Backward and forward trajectory calculations confirmed that volcanic smoke from the Sakurajima volcano was transported to the summit of Mt. Fuji.

Keywords: Mountain; Trace gas; Atmospheric pollutant; East Asia; Volcano.

INTRODUCTION

It is important to be aware of air quality on a regional scale. Polluted air originating from high emission areas can be transported to remote locations and can influence the air quality there. Also on site observation data at remote places are necessary for the validation of global or regional calculations and remote sensing observations.

O_3 is a significant short-lived trace gas. O_3 becomes high concentration in polluted urban areas through photochemical reactions, causing health risks for humans and vegetation. In addition, O_3 can be transported to remote rural areas. The concentrations of O_3, a short-lived tropospheric greenhouse gas, has been increasing in East Asia at a regional scale according to some reports (Akimoto, 2003; Tanimoto, 2009; Tanimoto *et al.*, 2009); high levels of O_3 can affect plant growth and decrease crop production. A regional and hemispheric increase of tropospheric O_3 causes a positive shift in radiative forcing. In recent years, regional transport has led to high concentrations of O_3 in Japan. For example, quite high photochemical oxidant (more than 120 ppbv) was observed in the western coastal areas where there is minimal human activity (Ohara *et al.*, 2008). On the other hand, there is a report that O_3 concentration have been decreased from 2008 at mountain site (Happo) in Japan (Okamoto *et al.*, 2015). More monitoring of O_3 at remotes will be required.

Monitoring CO at remote sites is also important to understand because this gas is a strong indicator of pollution. O_3 can be produced by photochemical reactions in the presence of NO_x and volatile organic compounds (VOCs), which work as peroxy radical sources, especially in polluted areas. NO_x is oxidized to HNO_3 and is removed from the atmosphere within a few days. In remote places, NO_x concentrations become quite low after transport. On the other hand, CO is emitted along with NO_x and VOCs during the process of combustion. The lifetime of CO is longer than one month so its concentration generally remains high even after being transported to remote locations. Therefore, monitoring of O_3 and CO concentrations provide useful information in understanding the long-range transport of

* Corresponding author.
Tel.: +81-42-677-2833; Fax: +81-42-677-2833
E-mail address: shungo@tmu.ac.jp

the polluted air to remote areas.

SO_2 is another atmospheric pollutant emitted from the combustion of fossil fuel. The main sources of SO_2 is the combustion of coal, a process highly common in China (Kurokawa *et al.*, 2013). Therefore measurement of SO_2 at remote sites can be useful to detect long range transport of polluted air (Igarashi *et al.*, 2004, 2006). In addition to anthropogenic emission, SO_2 is also emitted through volcanic activity. There are several volcanoes in Japan and some of them become active recently. SO_2 measurement would be important also to monitor volcanic activities.

Atmospheric pollutants are emitted near ground mostly and transported in the boundary layer along the ground and ocean. In addition, polluted air can also be lifted by convection and transported in long distance through the free troposphere. Most ground-based observatories are located at low altitudes, limiting the availability of onsite measurements in the free troposphere. Therefore, aircraft measurements are beneficial when measuring the transport of polluted air. Some intensive studies have been performed to observe the continental outflow of atmospheric pollutants to the East China Sea and the Pacific Ocean (Hoell *et al.*, 1997; Huebert *et al.*, 2003; Jacob *et al.*, 2003; Hatakeyama *et al.*, 2014). However, aircraft measurements are quite expensive and are only suitable for short-term observations. On the contrary, ground-based measurements at mountain sites are valuable for long-term observation at relatively low costs.

In East Asia, high-altitude measurements have been carried out at mountain sites, including Lulin Atmospheric Background Station in Taiwan (Wai *et al.*, 2008; Sheu *et al.*, 2010; Lee *et al.*, 2011; Ou-Yang *et al.*, 2012, 2014), Mt. Tai in China (Kanaya *et al.*, 2013 and references therein), Mt. Happo in Japan (Kajii *et al.*, 1998; Kato *et al.*, 2002; Pochanart *et al.*; 2004, Tanimoto, 2009), Mt. Norikura in Japan (Watanabe *et al.*, 1995; Minami and Ishizuka, 1996; Watanabe *et al.*, 1999; Osada *et al.*, 2002; Nishita *et al.*, 2008), Mt. Kiso-Komagatake in Japan (Zaizen *et al.*, 2014), and Mt. Tateyama in Japan (Osada *et al.*, 2003, 2009; Watanabe *et al.*, 2010; Watanabe and Honoki, 2013; Uehara *et al.*, 2015).

Mt. Fuji is a volcanic mountain in Japan, well known for its beauty, and was registered as a UNESCO (United Nations Educational, Scientific and Cultural Organization) World Heritage site in 2013. The Mt. Fuji weather station is located at the summit of Mt. Fuji and has been used as an important meteorological observatory. Because of its high elevation (3776 m a.s.l.) and absence of local pollution sources, the Mt. Fuji weather station is ideal for regional air quality measurements in the free troposphere.

Previously, various atmospheric measurements were carried out at the summit of Mt. Fuji; some of the reported results are available in literature. O_3 was observed in August 1992 (Tsutsumi et al, 1994, 1998), CO was observed during the summer of 1997 (Tsutsumi and Matsueda, 2000) and in 2004 (Igarashi *et al.*, 2006), and SO_2 was observed from October 2002 to July 2004 (Igarashi *et al.*, 2004, 2006); however, these continuous onsite measurements were stopped in 2004. In addition to these gasses, aerosols (Naoe *et al.*, 2003; Kaneyasu *et al.*; 2007, Suzuki *et al.*, 2008; 2010, Ueda *et al.*, 2014) and fog/rain water (Watanabe *et al.*, 2006; Wai *et al.*, 2008) were measured and reported.

Since East Asia is one of the most populated area, the regional atmospheric pollution would be reflected by economical and technological situations. Therefore update observed information of atmospheric pollutants at this region would be meaningful. This paper reports the observations of CO, O_3, and SO_2 concentrations carried out at Mt. Fuji during the summer of 2013.

OBSERVATIONS

Observation Site and Period

The Mt. Fuji weather station is located at the summit of Mt. Fuji (3776 m a.s.l., 35.4°N, 138.7°E), as shown in Fig. 1, and it is operated by the Japan Meteorological Agency. Especially, the mount Fuji radar system was famous and it worked as an important weather forecast and typhoon warning system in previous times. However, most modern meteorological observations shifted to be made through satellite remote sensing. In 2004, the Mt. Fuji weather station reduced its operations leaving only automated tools monitoring fundamental meteorological measurements. Since 2007, the non-profit organization "Valid Utilization of Mt. Fuji Weather Station the station" attempted to support activities at the Mt. Fuji weather station and it is available for scientific and educational purposes only during summer months. Some atmospheric measurements (CO, O_3, SO_2, CO_2, Hg, aerosol, fog/rain, radon etc.) have been conducted with their support.

For our study, instruments to monitor CO, O_3, and SO_2 were installed from July 18 to August 22, 2013. With the exception of electric power outage on July 23 and 24 caused by a thunderstorm approach, data were successfully collected during the entire measurement period.

Instruments

CO (Thermo Electron, Model 48C) and O_3 analyzers (Thermo Electron, Model 49i) were set up on the second floor of the main building at the Mt. Fuji weather station. Ambient air was collected through a PFA tube (O.D. 6.35 mm, I.D. 4 mm, about 10 m length) and transferred into these instruments. A Teflon filter and a PFA water trap were installed in the inlet tube because fog condensation (cloud water droplets) on the inlet tube could potentially be a serious problem at this observation site.

The CO analyzer employs non-dispersive infrared absorption for the assessment. The background signal of the CO monitor is influenced by temperature (CO signal decreases as temperature increases) and water vapor, and also increases gradually as the correlation wheel accumulates dirt. Therefore, frequent background signal checks are necessary for ambient air measurements at clean remote sites using zero air (CO removed from air), which is generated by a heated Pt catalyst (Thermo Electron Model 96). CO is oxidized to CO_2, but because the Pt converter does not remove water, the amount of water in the ambient air and zero air should be the same. Every hour, the zero air was measured from 0 to 15 min while ambient air was measured from 16

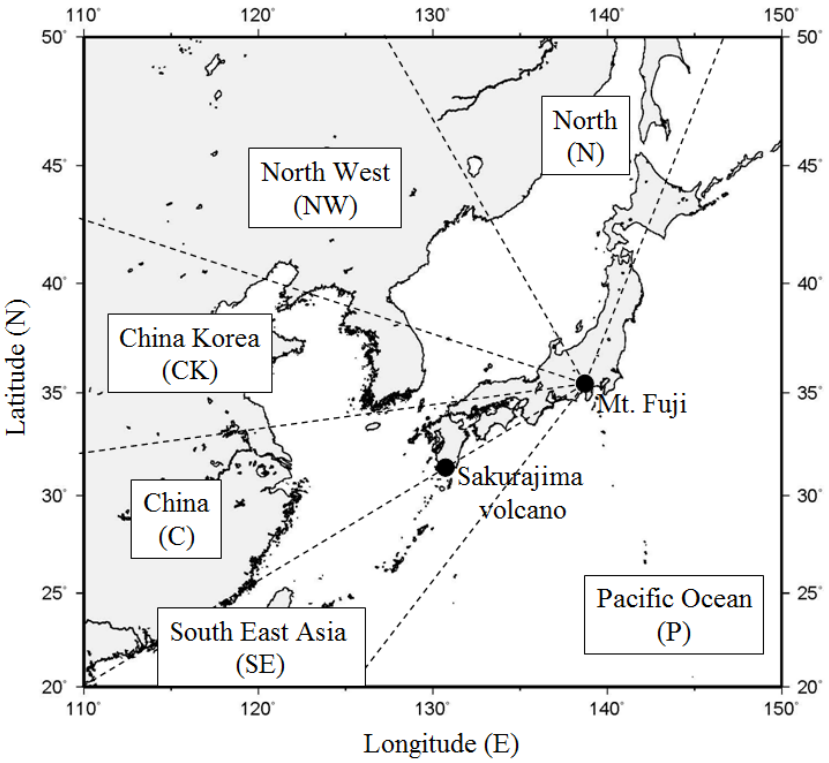

Fig. 1. Location of Mt. Fuji (35.4°N, 138.7°E) and Sakurajima volcano. Categorized areas for backward trajectory analysis are also shown.

to 59 min using an automatic switch of the solenoid valve in the CO analyzer. CO concentrations in the ambient air can be obtained by subtracting data during zero air measurements from the data during ambient air measurements. Noting that the air temperature of the observatory was not controlled to be constant. During the measurement period the CO instrument reading of zero air was about 100 ppb initially and increased to about 1500 ppb, with roughly 200 ppb diurnal variation. The CO analyzer was calibrated by standard CO gas (Taiyo Nissan, Japan, 1.96 ppm) in the laboratory before and after field measurements without onsite calibration. Since the measurement principal is based on infrared absorption, decrease of the density of the molecules in high altitude (low pressure) influences the observed signal. However, we can assume ideal gas in ambient CO measurement and the instrument has a function to correct the pressure and temperature differences in the absorption cell. These corrections convert the observed mixing ratio to standard pressure and temperature conditions. Using the standard deviation during zero gas measurement on site, the detection limit of the CO analyzer in this measurement campaign was estimated to be 22.6 ppb.

The working principle of the O_3 analyzer is based on UV absorption. The O_3 analyzer was calibrated by an O_3 primary standard (Model 49i-PS) before field measurements (about 2 month before). Similar to the CO instrument, the observed O_3 mixing ratio was corrected to standard pressure and temperature conditions. The detection limit and uncertainty of the O_3 analyzer were 1 ppb and 1%, respectively, according to the company information.

The SO_2 analyzer (Thermo Electron, Model 43C-TL) was set up at another building of the Mt. Fuji weather station. Ambient air was drawn in from an air inlet chimney (I.D. 100 mm) at a high flow rate (143 L min^{-1}) and separated in a PFA tube (O.D. 6.35 mm, I.D. 4 mm) leading to the SO_2 analyzer. Similar to the CO measurement process, zero air produced by catalyst (SP Blend Media, Purafil) and SO_2 in ambient air were measured periodically. The analyzer was calibrated before and after the field measurements using standard SO_2 gas (Takachiho, Japan, 0.98 ppm), diluted by mass flow controllers. The detection limit of the SO_2 monitor was documented as 0.5 ppbv (for 300 sec) in the manual from the company, but from the actual measurements in our system, the detection limit was estimated to be an hourly average of 0.06 ppbv. Igarashi *et al.* (2004) used the same commercial SO_2 analyzer (Model 43C-TL), but their inlet system was different from ours. They carefully tested the performance of the SO_2 measurement system and concluded that the detection capability was 0.05 ppbv.

The output analog signal of these instruments was converted to digital data by U3-HV (Labjack) and was logged on a personal computer at intervals of one minute. The data logging computers were attached to the network at the Mt. Fuji weather station connected to the Internet with the wireless LAN provided by the National Institute of Radiological Sciences. The real-time data could then be verified by a remote control system from any location, which was beneficial considering the observatory was not easily accessible. The electric power supply to the Mt. Fuji weather station needed to be shut down during an expected

thunderstorm to avoid fatal damages, and we ensured the instruments successfully restarted after electric power came back.

Backward Trajectory Calculation

Backward trajectories were calculated using the NOAA HYSPLIT 4 model (Draxler and Rolph, 2012; Rolph, 2012). The air mass was traced back 5 days (120 h) and calculated at intervals of 4 h. A meteorological data set was used for GDAS along with model vertical velocity data for vertical motion. The initial elevation reading by the backward trajectory calculation was 3776 m. These readings are categorized based on different origins, as: North (N), North West (NW), China Korea (CK), China (C), South East Asia (SE), and Pacific Ocean (P) as shown in Fig. 1. Trajectories that were difficult to categorize are named unclassified (U). Because of the problems with the power supply, no CO, O_3 and SO_2 data were available during thunderstorm approach; a total of 194 backward trajectory calculations were thus obtained.

RESULTS AND DISCUSSION

CO and O_3 Results

Hourly mean CO and O_3 concentrations are shown in Fig. 2. Even in a remote location at a high altitude, there were considerable variations in the concentrations of both CO and O_3. Average CO and O_3 concentrations and standard deviations were 105.9 ± 44.3 ppbv and 29.3 ± 13.2 ppbv for CO and O_3, respectively. The variation of CO and O_3 concentrations during the summer of 2013 is consistent with previous recordings by Tsutsumi and Matsueda (2000). Tsutumi *et al.* (1994) reported the standard deviation of O_3 concentration to be low during the winter but high during the summer.

The top of Mt. Fuji reaches the free troposphere where local sources of emissions are not expected. Therefore, generally, it is safe to assume that the large variations in CO and O_3 concentrations originate from transport from a distant air mass. However, Tsutsumi and Matsueda (2000) described that the air at the top of the Mt. Fuji was influenced in some cases by emissions from Nagoya, a large city in Japan. Fig. 2 shows the origin of air masses plotted through backward trajectories. Usually during summer months air from the Pacific Ocean is dominant. However, during the observation period in the summer of 2013 only about 10% of transported air originated from the Pacific Ocean. It can be observed that CO and O_3 concentrations are low when the air masses originate from P or SE. Average concentrations and standard deviations of pollutants in the air masses of different origins are summarized in Table 1. Air masses originating from CK, NW, and N show the highest average concentrations of CO and O_3, while air masses from SE, and P show lower concentrations. The category of C was observed only 1.5% frequency and was considered statistically unreliable. A close analysis of the results showed that CK and NW had almost the same average O_3 concentrations, but CO was higher for NW. SE and P had similar average O_3 concentrations, while SE showed a higher CO concentration. However their differences were within standard deviation, it is interesting to note that SE and P show differences in CO, which is emitted primary from combustion sources, yet there is almost the same concentration of O_3 which is

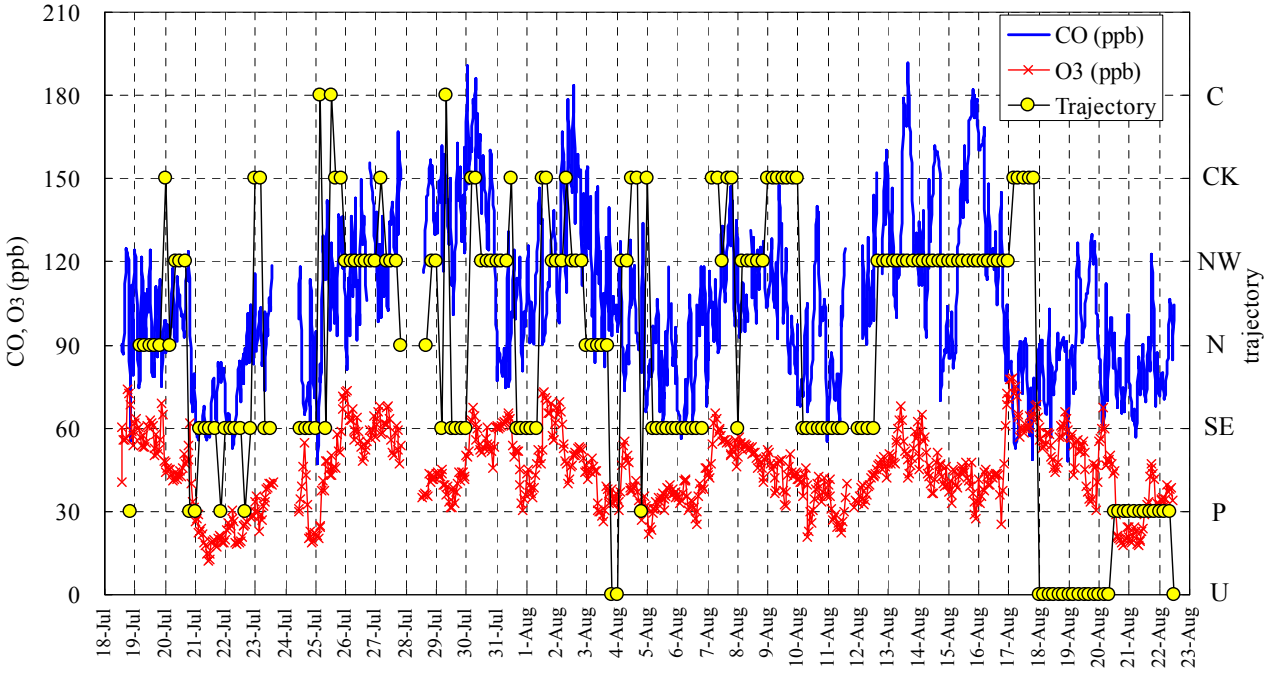

Fig. 2. Time series of observed CO and O_3 (hourly mean data) during the summer of 2013. Air mass origin determined by backward trajectory is also plotted (right axis). N: North, NW: North West, CK: China Korea, C: China, SE: South East Asia, P: Pacific Ocean, U: unclassified.

Table 1. Average and standard deviation of CO and O_3 for each backward trajectory category.

	CO average ppbv	CO stdev ppbv	O_3 average ppbv	O_3 stdev ppbv	Frequency %
China (C)	114.5	33.9	36.9	12.9	1.5
China Korea (CK)	101.8	24.6	50.8	11.4	16.0
North West (NW)	126.6	26.3	50.5	8.8	31.4
North (N)	112.4	23.9	46.7	10.3	6.7
South East Asia (SE)	92.8	26.2	33.7	9.5	25.8
Pacific Ocean (P)	80.5	14.6	33.0	14.4	9.3
Unclassfied (U)	93.0	15.9	50.0	8.5	9.3

stdev: standard deviation.

produced through secondary reactions.

In Fig. 3, a scatter plot of CO and O_3 is shown by different symbols for air mass origins categorized by backward trajectory. Relatively polluted air masses (N, NW, CK, and C) are shown in left panel and relatively cleaner air masses (P and SE) are shown in right panel. It can be seen that low CO and O_3 concentrations mostly originated from P and SE, while high CO and O_3 concentrations mostly originated from CK, NW, and N. In the P and SE plots, there is a rough linear correlation between CO and O_3 (shown in Fig. 3) To support the comparison of different figures, "guide line" was shown in Fig. 3. The guide line passes on typical oceanic clean air (50 ppb CO and 10 ppb O_3) and continental air (assumed to 150 ppb CO and 55 ppb O_3). In relatively clean air masses, influence of polluted continental air to the clean air would make this linear correlation. In the N, NW, CK, and C plots, there is greater variation and it is difficult to see a linear correlation as observed in P and SE (guide line). Higher CO with lower O_3 concentrations were observed in NW. These deviated data would be related to less photochemical production of O_3.

Some data from of CK, NW, and N were clearly deviated from a linear correlation between CO and O_3 (low CO but high O_3). Because the observatory is at high elevation, the air from high altitudes (stratosphere) is more easily transported. Tsutsumi *et al.* (1998) reported a stratospheric O_3 intrusion event at the summit of Mt. Fuji. Since CO is mainly emitted from the sources on ground (fossil fuel combustion, biomass burning etc.), CO concentrations are generally higher near ground and lower at high altitudes. On the contrary, O_3 is higher near the stratosphere where the ozone layer exists. Most of the low CO with high O_3 data observed here were originated from high altitudes in the backward trajectory calculations. However, the air masses originating from high altitude were not always clean and some contain generally polluted air (high CO and high O_3). Since air temperature decreases with altitude and water is removed as cloud droplets, water vapor decreases with altitude; therefore, water vapor content is important when confirming the influence of high altitude air. In Fig. 4, a time series of CO, O_3, and water vapor content (observed by the Japan Meteorological Agency) are shown together. There are periods when the water content is quite low, and O_3 becomes higher while CO concentrations decrease. In Fig. 5, the correlation of CO and O_3 is plotted with different symbols for water content (low water vapor plotted in warm colors and high water vapor plotted in cold colors). It is clear that most of the low CO and high O_3 data contain low water and they would be transported from high altitudes. These data verify that influence of stratospheric air can be observed at high-

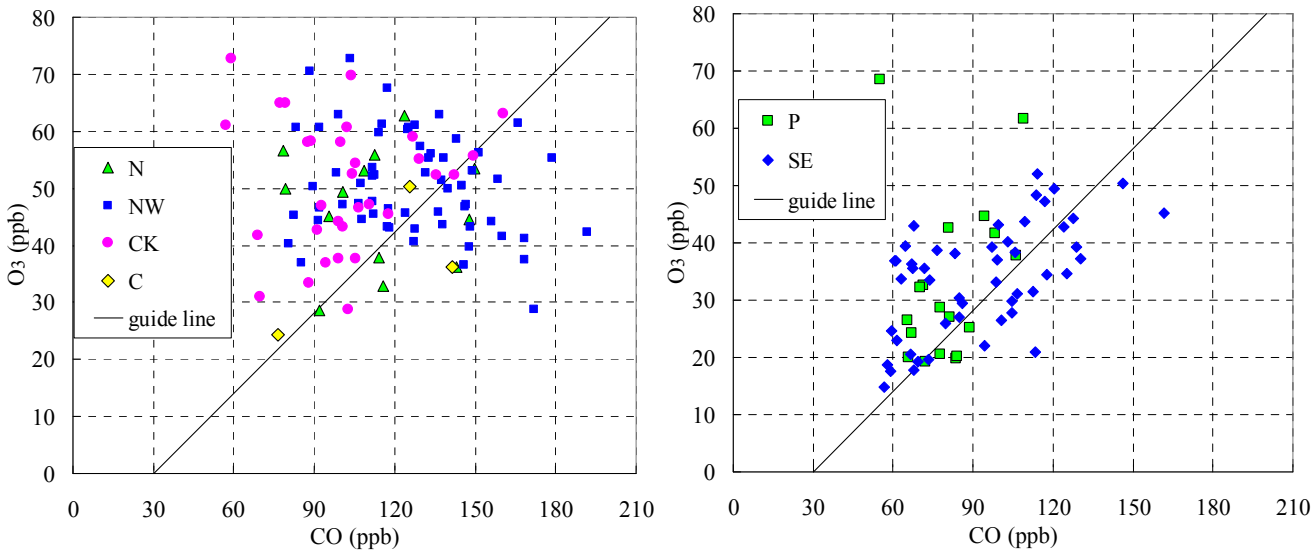

Fig. 3. Correlation plots of hourly mean CO and O_3 data for N, NW, CK, and C air masses (left) and for P and SE air masses (right). Guide lines assumed mixing of clean oceanic and polluted continental air are shown in both panels.

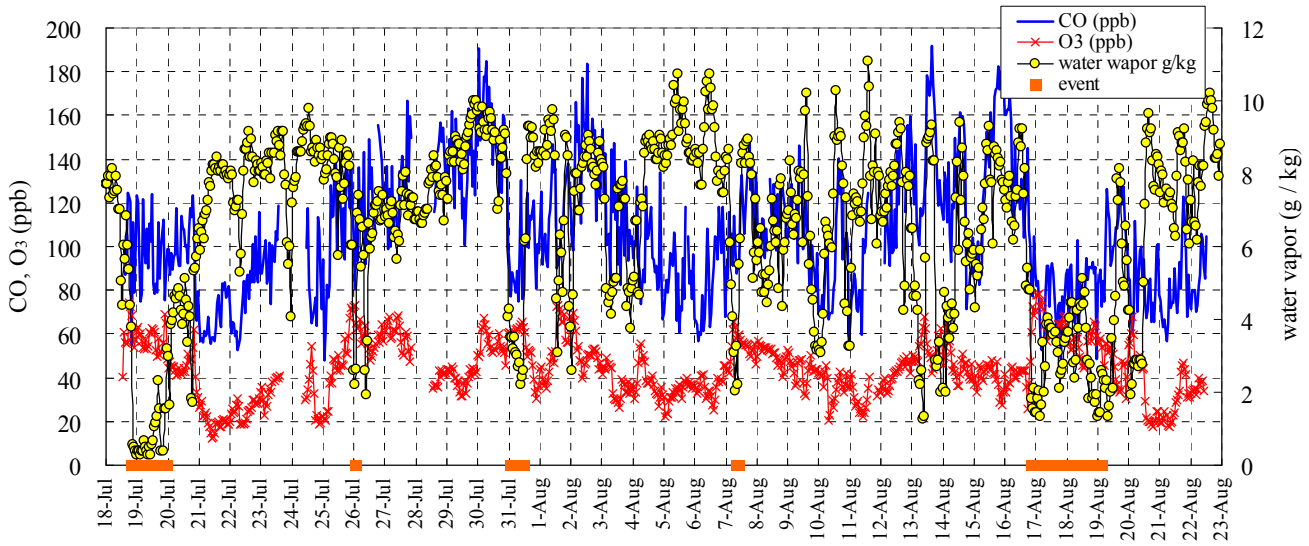

Fig. 4. Time series of water vapor (right axis) with hourly mean CO and O_3 (left axis). Very low water vapor were observed. The period of the "event", high O_3, low CO, low water vapor event (O_3 > 50 ppb, CO < 90 ppb, water < 4 g kg^{-1}), was shown on x-axis.

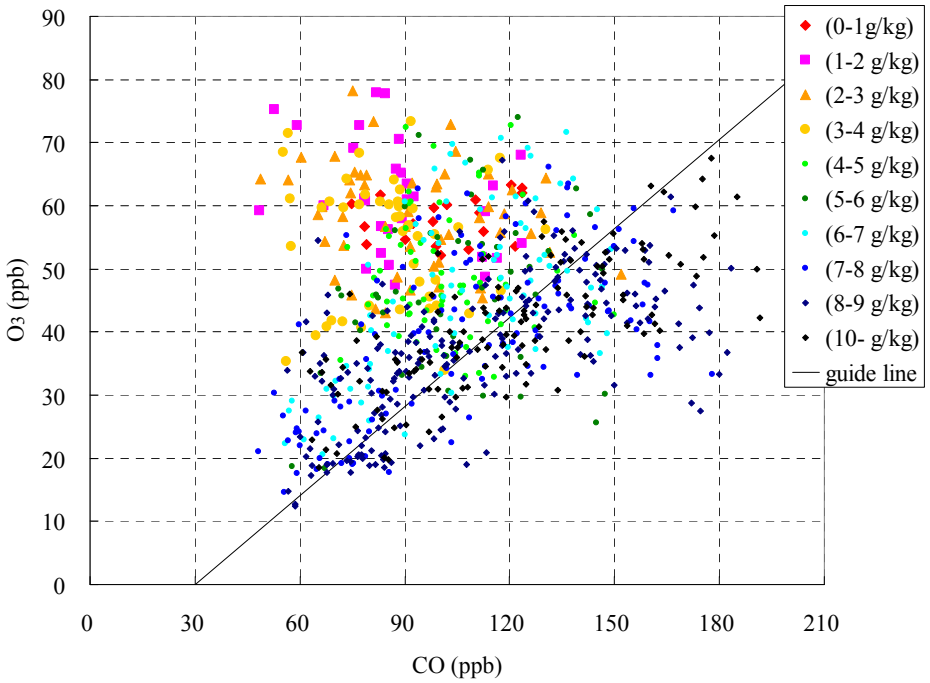

Fig. 5. Correlation between hourly mean CO and O_3 plotted by different symbols for water vapor content. The data with low CO and high O_3 had lower water vapor, indicating influenced by tropospheric air. The guide line in Fig. 3 is also shown by a solid line.

elevation observatories such as Mt. Fuji, even during the summer. These high O_3, low CO, low water vapor data are named as "event" here. From Fig. 5, the "event" was defined as O_3 > 50 ppb, CO < 90 ppb, water < 4 g kg^{-1}. The "event" was found 67 hours during total measurement period (864 hours). The period of the "event" was shown in Fig. 4. From Fig. 5, it can be also seen that relatively higher CO data tend to appear with higher water vapor content. High CO with low O_3 data would be influenced by local pollution sources. But it can also be explained as polluted air without enough photochemical reaction for O_3 production. High water content would be related to rainy conditions with less sunlight, and the observed high CO but low O_3 air would be tended to have higher water content.

SO_2 Results

SO_2 concentrations were mostly below the detection limit of the SO_2 analyzer (0.06 ppbv) during the measurement

period (not shown). This is consistent with Igarashi *et al.* (2004), when they reported SO_2 concentrations were lower than the detection limit of their instrument during the summer. On August 20–21, however, an increase in the concentration of SO_2. was observed. Fig. 6 shows one-minute averages during this high SO_2 event. The combustion of fossil fuels, especially coal, is the main source of SO_2 emissions. Igarashi *et al*. (2004, 2006) observed episodic SO_2 spikes, especially from January to April. In their high SO_2 events, CO and ^{222}Rn (indicator of ground surface sources) increased, and they identified episodic high SO_2 through long-range transport of pollutants from the Asian continent where coal consumption is high. In Japan, anthropogenic SO_2 emissions are carefully controlled, except from the emissions of sea vessels. If polluted air from fossil fuel combustion sources is transported to the top of Mt. Fuji, the concentration of CO is expected to be high. During the high SO_2 event on August 20–21, however, CO concentration (9 min average data) did not increase as shown in Fig. 6. Also O_3 concentration did not fluctuate during the high SO_2 event Therefore, SO_2 transported from fossil fuel combustion is not a suitable explanation for this high SO_2 event.

Volcanoes are another source of SO_2 emissions and there are several active volcanoes in Japan. Miyake-jima, which is 170 km south of Mt. Fuji, erupted in July 2000 when aerosol (Naoe *et al.*, 2003) and SO_2 (Igarashi *et al.*, 2004) were observed from its volcanic plume at the summit of Mt. Fuji. Recently, Sakurajima volcano (Fig. 1, about 820 km away from Mt. Fuji) has become active and its plume was detected at a distant ground site (Noto peninsula) in Japan (Watanabe *et al.* 2015). Especially, there was a massive eruption and the volcanic ash rose to around 5000 m in altitude at 16:31 on August 18, 2013. Fig. 7 shows backward trajectories (a) and forward trajectories (b) during the high SO_2 event. For the backward trajectories, the starting altitudes were 4276, 4026, and 3776 m a.s.l., considering the uncertainty in backward trajectory calculations. The highest altitude trajectory passed over the Sakurajima volcano. For the forward trajectories, the starting altitude was selected as 3000 m and the starting time was at 10:00, 13:00, 15:00 and 18:00 on August 18. These air masses from Sakurajima arrived near Mt. Fuji around August 20–21, and this is consistent with the observation. Because Sakurajima volcano was quite active and erupted several times at that time (144 times eruptions were observed in one month on August in 2013), slight difference of the starting time and the assumption using the starting altitude at 3000 m for the forward trajectories will be not critical issues. At the same time of the high gaseous SO_2 peak, aerosol compositions indicated the influence of a volcanic plume (Ogata *et al.*, paper in preparation). Therefore, it is reasonable to conclude that the plume from the Sakurajima volcano is related to observations at the top of Mt. Fuji during the high SO_2 event on August 20–21.

In Japan, there are several active volcanoes contributing to air pollution. In addition to these volcanoes there are various other natural sources of atmospheric trace species that can be observed at high altitudes. For example, smoke emissions from fires in the Siberian Forest during 2003 were observed from the summit of Mt. Fuji (Kaneyasu *et al.*, 2007). Indeed, atmospheric monitoring at high-altitude mountain sites is useful in observing air quality.

CONCLUSION

We observed CO, O_3 and SO_2 concentrations at the summit of Mt. Fuji during the summer of 2013. CO and O_3 showed roughly similar variation in their concentrations, which can be explained by the air mass exchange between clean oceanic air and polluted continental air. Low CO and high O_3 were also observed in some cases when water vapor content in the air was low, indicating the influence of

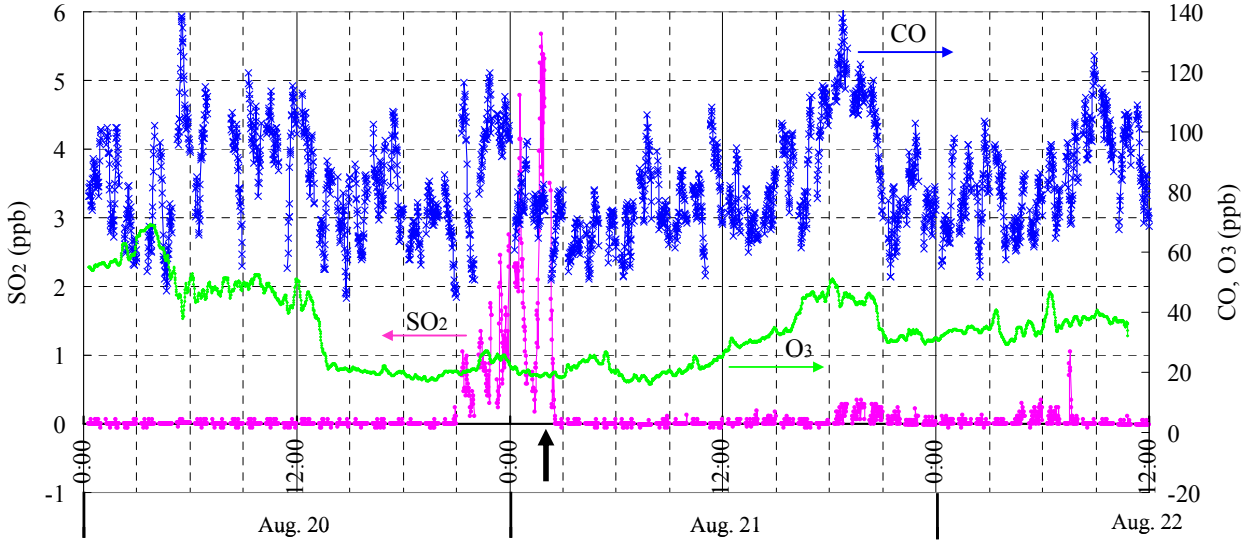

Fig. 6. Time series of SO_2 data (1 min average, left axis), CO and O_3 data (9 min average, right axis) around the high SO_2 period on August 20–21. The initial time of backward trajectory in Fig. 7 is indicated by a bold arrow. The time format is local time (JST).

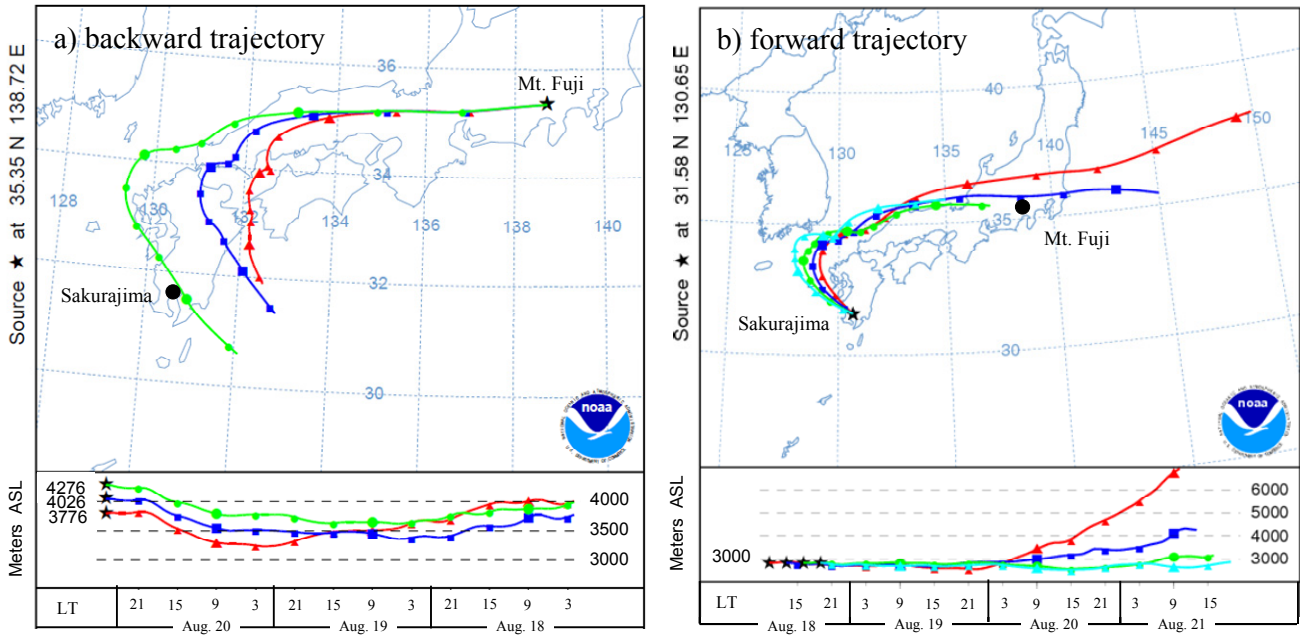

Fig. 7. (a) Backward trajectories during high SO_2 at the summit of Mt. Fuji (2:00 August 21, 2013 LT). The results of three different altitude (4276, 4026, 3776 m a.s.l.) are shown. Backward trajectory was passed over Sakurajima volcano before arriving Mt. Fuji. (b) Forward trajectory around the huge eruption of Sakurajima volcano. Starting times were at 10:00, 13:00, 15:00, and 18:00 on August 18, 2013. Altitude was selected at 3000 m.

stratospheric air. High SO_2 peaks were observed, which were identified as the volcanic plume of the Sakurajima volcano, located 820 km away. It is indeed evident that atmospheric observations taken at high-altitude mountain sites will be useful in monitoring regional ambient air in the free troposphere, including transport and intrusion events.

ACKNOWLEDGEMENTS

We greatly appreciate the staff of the Mt. Fuji weather station and the members of the non-profit organization, Valid Utilization of Mt. Fuji Weather Station, especially Prof. Yukiko Dokiya for supporting the field measurements. We want to thank to Dr. Kazuaki Yajima at the National Institute of Radiological Sciences for providing a wireless LAN connection at the Mt. Fuji weather station. We also want to thank the Japan Meteorological Agency for allowing us to alter the Mt. Fuji weather station for our project and for providing meteorological data. This work was partly supported by the joint research program of the Solar-Terrestrial Environmental Laboratory, Nagoya University and by JSPS KAKENHI (Grant No. 25340017).

REFERENCES

Akimoto, H. (2003). Global air quality and pollution. *Science* 302: 1716–1719.

Draxler, R.R. and Rolph G. D. (2012). HYSPLIT (Hybrid Single-Particles Lagrangian Integrated Trajectory) Model access via NOAA ARL READY Website (http://ready.arl.noaa.gov/HYSPLIT.php), NOAA Air Resources Laboratory, Silver Spring, MD.

Hatakeyama, S., Ikeda, K., Hanaoka, S., Watanabe, I., Arakaki, T., Bandow, H., Sadanaga, Y., Kato, S., Kajii, Y., Zhang, D., Okuyama, K., Takashi, T., Fujimoto, N., Seto, T., Shimizu, A., Sugimoto, N. and Takami, A. (2014). Aerial observations of air masses transported from East Asia to the western pacific: Vertical structure of polluted air masses. *Atmos. Environ.* 97: 456–461.

Hoell, J.M., Davis, D.D., Liu, S.C., Newell, R.E., Akimoto, H., McNeal, R.J. and Bendura R.J. (1997). The pacific exploratory mission-west phase B: February-March, 1994. *J. Geophys. Res.* 102: 28223–28239.

Huebert B.J., Bates, T., Russell, P.B., Shi, G., Kim, Y.J., Kawamura, K., Carmichael, G. and Nakajima, T (2003). An overview of ACE-Asia: strategies for quantifying the relationships between Asian aerosols and their climatic impacts. *J. Geophys. Res.* 108: D23.

Igarashi, Y., Sawa, Y., Yoshioka, K., Matsueda, H., Fujii, K. and Dokiya, Y. (2004). Monitoring the SO_2 concentration at the summit of Mt. Fuji and acomparison with other trace gases during winter. *J. Geophys. Res.* 109: D17304.

Igarashi, Y., Sawa, Y., Yoshioka, K., Takahashi, H., Matsueda, H. and Dokiya, Y. (2006). Seasonal variations in SO_2 plume transport over Japan: Observations at the summit of Mt. Fuji from winter to summer. *Atmos. Environ.* 40: 7018–7033.

Jacob, D.J., Crawford, J.H., Kleb, M.M., Connors, V.S., Bendura, R.J., Raper, J.L., Sachse, G.W., Gille, J.C., Emmons, L. and Heald, C.L. (2003). Transport and chemical evolution over the Pacific (TRACE-P) aircraft mission: Design, execution, and first results. *J. Geophys. Res.* 108: D20.

Kajii, Y., Someno, K., Tanimoto, H., Hirokawa, J., Hajime, A., Katsuno, T. and Kawara, J. (1998). Evidence for the seasonal variation of photochemical activity of tropospheric ozone: Continuous observation of ozone and CO at Happo, Japan. *Geophys. Res. Lett.* 25: 3505–3508.

Kanaya, Y., Akimoto, H., Wang, Z.F., Pochanart, P., Kawamura, K., Liu, Y., Li, J., Komazaki, Y., Irie,, H., Pan, X.L., Taketani, F., Yamaji, K., Tanimoto, H., Inomata, S., Kato, S., Suthawaree, J., Okuzawa, K., Wang, G., Aggarwal, S.G., Fu, P.Q., Wang, Y. and Zhuang, G. (2013). Overview of the Mt. Tai experiments (MTX2006) in Central East China in June 2006: Studies of significant regional air pollution. *Atmos. Chem. Phys.* 13: 8265–8283.

Kaneyasu, N., Igarashi, Y., Sawa, Y., Takahashi, H. Takada, H. Kumata, H. and Holler, R. (2007). Chemical and optical properties of 2003 Siberian forest fire smoke observed at the summit of Mt. Fuji, Japan. *J. Geophys. Res.* 112: D13214.

Kato, S., Pochanart, P., Hirokawa, J., Kajii, Y., Akimoto, H., Ozaki, Y., Obi, K., Katsuno, T., Streets, D.G. and Minko, N.P. (2002). The influence of Siberian forest fires on carbon monoxide concentrations at Happo, Japan. *Atmos. Environ.* 36: 383–388.

Kurokawa, J., Ohara, T., Morikawa, T., Hanayama, S., Janssens-Maenhout, G., Fukui, T., Kawashima, K. and Akimoto, H. (2013). Emissions of air pollutants and greenhouse gases over Asian regions during 2000–2008: Regional emission inventory in Asia (REAS) version 2. *Atmos. Chem. Phys.* 13: 11019–11058.

Lee, C.T., Chuang, M.T., Lin, N.H., Wang, J.L., Sheu, G.R., Chang, S.C., Wang, S.H., Huang, H., Chen, H.W., Liu, Y.L., Weng, G.H. and Hsu, S.P. (2011). The enhancement of $PM_{2.5}$ mass and water-soluble ions of biosmoke transported from Southeast Asia over the Mountain Lulin site in Taiwan. *Atmos. Environ.* 45: 5784–5794.

Minami, Y. and Ishizaka, Y. (1996). Evaluation of chemical composition in fog water near the summit of a high mountain in Japan. *Atmos. Environ.* 30: 3363–3376.

Naoe, H., Heintzenberg, J., Okada, K., Zaizen, Y., Hayashi, K., Tateishi, T., Igarashi, Y., Dokiya, Y. and Kinoshita, K. (2003). Composition and size distribution of submicrometer aerosol particles observed on Mt. Fuji in the volcanic plumes from Miyakejima. *Atmos. Environ.* 37: 3047–3055.

Nishita, C., Osada, K., Kido, M., Matsunaga, K. and Iwasaka, Y. (2008). Nucleation mode particles in upslope valley winds at Mount Norikura, Japan: Implications for the vertical extent of new particle formation events in the lower troposphere. *J. Geophys. Res.* 113: D06202.

Ohara, T., Uno, I., Kurokawa, J., Hayasaki, M. and Shimizu, A (2008). Episodic pollution of photochemical ozone during 8–9 May 2007 over Japan - Overview-. *J. Jpn. Soc. Atmos. Environ.* 43: 198–208 (in Japanese).

Okamoto, S., Tanimoto, H., Nara, H., Ikeda, K. and Yamaji, K. (2015). Observations of O_3, CO, CO_2 and CH_4 concentrations at Happo and estimations of the source by chemical transport model. Abstract of Japan Geoscience Union Meeting 2015, AAS21-13 (in Japanese).

Osada, K., Kido, M., Nishita, C., Matsunaga, K., Iwasaka, Y., Nagatani, M. and Nakada, H. (2002), Changes in ionic constituents of free tropospheric aerosol particles obtained at Mt. Norikura (2770 m a.s.l.), central Japan, during the Shurin period in 2000. *Atmos. Environ.* 36: 5469–5477.

Osada, K., Kido, M., Iida, H., Matsunaga, K., Iwasaka, Y., Nagatani, M. and Nakada, H. (2003). Seasonal variation of free tropospheric aerosol particles at Mt. Tateyama, central Japan. *J. Geophys. Res.* 108: D23, 8667.

Osada K., Ohara T., Uno I., Kido M. and Iida H. (2009). Impact of Chinese anthropogenic emissions on submicrometer aerosol concentration at Mt. Tateyama, Japan. *Atmos. Chem. Phys.* 9: 9111–9120.

Ou-Yang, C.F., Lin, N.H., Sheu, G.R., Lee, C.T. and Wang, J.L. (2012). Seasonal and diurnal variations of ozone at a high-altitude mountain baseline station in East Asia. *Atmos. Environ.* 46: 279–288.

Ou-Yang, C.F., Lin, N.H., Lin, C.C., Wang, S.H., Sheu, G.R., Lee, C.T., Schnell, R.C., Lang, P.M., Kawasato, T. and Wang, J.L. (2014). Characteristics of atmospheric carbon monoxide at a high-mountain background station in East Asia. *Atmos. Environ.* 89: 613–622.

Pochanart, P., Kato, S., Katsuno, T. and Akimoto, H. (2004). Eurasian continental background and East Asian regionally polluted levels of ozone and CO in northeast Asia. *Atmos. Environ.* 38/39: 1325–1336.

Rolph, G.D. (2012). Real-time environmental applications display system (READY) Website (http://ready.arl.noaa.gov). NOAA Air Resources Laboratory, Silver Spring, MD.

Sheu, G.R., Lin, N.H., Wang, J.L., Lee, C.T., Ou-Yang, C.F. and Wang, S.H. (2010). Temporal distribution and potential sources of atmospheric mercury measured at a high-elevation background station in Taiwan. *Atmos. Environ.* 44: 2393–2400.

Suzuki, I., Hayashi, K., Igarashi, Y., Takahashi, H., Sawa, Y., Ogura, N., Akagi, T. and Dokiya, Y. (2008) Seasonal variation of water-soluble ion species in the atmospheric aerosols at the summit of Mt. Fuji. *Atmos. Environ.* 42: 8027–8035.

Suzuki, I., Igarashi, Y., Dokiya, Y. and Akagi, T. (2010). Two extreme types of mixing of dust with urban aerosols observed in Kosa particles: "After" mixing and "on-the-way" mixing. *Atmos. Environ.* 44: 858–866.

Tanimoto, H. (2009). Increase in springtime tropospheric ozone at a mountainous site in Japan for the period 1998–2006. *Atmos. Environ.* 43: 1358–1363.

Tanimoto H., Ohara, T. and Uno, I. (2009). Asian anthropogenic emissions and decadal trends in springtime tropospheric ozone over Japan: 1998–2007. *Geopys. Res. Lett.* 36: L23802.

Tsutsumi, Y., Zaizen, Y. and Makino, Y. (1994). Tropospheric ozone measurement at the top of Mt. Fuji. *Geophys. Res. Lett.* 21: 1727–1730.

Tsutsumi, Y., Igarashi, Y., Zaizen, Y. and Makino, Y. (1998). Case studies of tropospheric ozone events observed at the summit of Mount Fuji. *J. Geophys. Res.* 103: 16935–16951.

Tsutsumi, Y. and Matsueda, H. (2000). Relationship of ozone and CO at the summit of Mt. Fuji (35.35°N, 138.73°E, 3776 m above sea level) in summer 1997. *Atmos. Environ.* 34: 553–561.

Ueda, S. Hirose, Y. Miura, K. and Okochi, H. (2014). Individual aerosol particles in and below clouds along a Mt. Fuji slope: Modification of sea-salt-containing particles by in-cloud processing. *Atmos. Res.* 137: 216–227.

Uehara, Y., Kume, A., Chiwa, M., Honoki, H., Zhang, J. and Watanabe, K. (2015). Atmospheric deposition and interactions with Pinus pumila regal canopy on Mt. Tateyama in the Northern Japanese Alps. *Arct. Antarct. Alp. Res.* 47: 389–399.

Wai, K.M., Lin, N.H., Wang, S.H. and Dokiya, Y. (2008). Rainwater chemistry at a high-altitude station, Mt. Lulin, Taiwan: Comparison with a background station, Mt. Fuji. *J. Geophys. Res.* 113: D06305.

Watanabe, K., Takebe, Y., Sode, N., Igarashi, Y., Takahashi, H. and Dokiya. Y. (2006). Fog and rain water chemistry at Mt. Fuji: A case study during the September 2002 campaign. *Atmos. Res.* 82: 652–662.

Watanabe, K., Ishizaka, Y. and Tanaka, H. (1995). Measurements of atmospheric peroxides concentrations near the summit of Mt. Norikura in Japan. *J. Meteorolog. Soc. Jpn.* 73: 1153–1160.

Watanabe, K., Ishizaka, Y. and Takenaka, C. (1999). Chemical composition of fog water near the summit of Mt. Norikura in Japan. *J. Meteorolog. Soc. Jpn.* 77: 997–1006.

Watanabe, K., Honoki, H., Iwai, A., Tomatsu, A., Noritake, K., Miyashita, N., Yamada, K., Yamada, H., Kawamura, H. and Aoki, K.. (2010). Chemical characteristics of fog water at Mt. Tateyama, near the coast of the Japan Sea in central Japan. *Water Air Soil Pollut.* 211: 379–393.

Watanabe, K. and Honoki, H. (2013). Measurements of aerosol number concentrations and rainwater chemistry at Mt. Tateyama, near the coast of the Japan sea in central Japan: On the influence of high-elevation Asian dust particles in autumn. *J. Atmos. Chem.* 70: 115–129.

Watanabe, K., Yamazaki, N., Mizuochi, R., Iwamoto, Y., Matsuki, A., Sadanaga, Y., Bandow, H. and Iwasaka, Y. (2015). High concentrations of sulfur dioxide and sulfate particles observed in Suzu City, the Noto Peninsula in late July 2012: On the influence of the smoke of Sakurajima. *Tenki* 62: 201–208 (in Japanese).

Zaizen, Y., Naoe, H., Takahashi, H. and Igarashi, Y. (2014). Number concentrations and elemental compositions of aerosol particles observed at Mt. Kiso-Komagatake in central Japan, 2010–2013. *Atmos. Environ.* 90: 1–9.

Received for review, November 18, 2015
Revised, February 25, 2016
Accepted, March 4, 2016